Challenge Journal of Structural Mechanics

Research Article

Investigation of influence of concrete material models on cyclic inelastic response of a concrete filled composite plate shear wall

Erkan Polat [a,*]

[a] *Department of Civil Engineering, Munzur University, 62000 Tunceli, Turkey*

ABSTRACT

A previously benchmarked finite element model of a previously tested composite plate shear wall-concrete filled (C-PSW/CF) was used to investigate the influence of three concrete material models on in-plane cyclic inelastic wall response, using LS-Dyna. The concrete material models considered were the Winfrith, KCC and CSCM, all available in LS-Dyna. Wall moment hysteresis, using the three concrete material models, were obtained and compared. Individual contribution of the steel and concrete to total base moment was investigated for each wall with the three concrete material models. The numerical results obtained using the KCC and CSCM were compared against the benchmarked results obtained using the Winfrith concrete material model. Moment contribution of the steel web and the steel boundary on total base moment of the steel part of the wall and moment contribution of the concrete web and concrete boundary on total base moment of the concrete part of the wall were individually investigated. The wall models with the KCC and CSCM concrete models were observed to cannot capture wall pinching which was captured by the Winfrith concrete model. The wall strength was overpredicted by the CSCM concrete model and predicted reasonably by the KCC concrete model. Average axial stress distribution of the infill concrete was obtained to investigate wall neutral axis and the maximum attained concrete strength using the three concrete models. Concrete axial stress distribution showed some level of confinement for the concrete models considered.

ARTICLE INFO

Article history:
Received 20 November 2019
Revised 25 December 2019
Accepted 8 January 2020

Keywords:
Concrete filled composite plate shear wall
Cyclic response
Finite element analysis
LS-Dyna

1. Introduction

Composite plate shear wall–concrete filled (C-PSW/CF) consists of steel skin plates filled with concrete (AISC 2016). C-PSW/CF can be used with or without boundary elements. The boundary elements can consist of either circular or half-circular concrete filled tubes as stipulated by AISC (2016). In C-PSW/CF steel web plates are interconnected (in the transverse direction) by tie bars that are distributed at a specified spacing along the width and height of the wall. Tie bars help stabilize the empty wall module during construction and provide resistance for the concrete casting pressure. Additionally, the steel-concrete composite action is achieved by the shear and axial force transfer at the steel-concrete interface by the tie bars.

C-PSW/CF is a promising alternative to conventional reinforced concrete shear walls. It offers advantages in terms of construction cost and time (steel plates are prefabricated and allows modular construction on site). For this type of shear walls, steel modules provide formwork, and at the same time serve as falsework (Varma et al., 2019). Outer steel modules provide reinforcement (in both transverse and longitudinal direction) so that shear and flexural rebar usage are eliminated (helps speed up the construction schedule and reduce on-site labor for any rebar related work). This type of shear walls has high flexural capacity and ductility, and popular in mid-rise to high-rise buildings located in seismic regions (Polat and Bruneau, 2017). These type of wall systems have been used in some high-rise buildings, including Rainer Square Tower in Seattle, China World Trade Center.

* *Corresponding author*. Tel.: +90-428-213-1794 ; E-mail address: erkanpolat@munzur.edu.tr (E. Polat)
ISSN: 2149-8024 / DOI: https://doi.org/10.20528/cjsmec.2020.02.006

Finite element methods have been widely used to investigate C-PSW/CF for their seismic performance. Advanced finite element programs, such as ABAQUS (Hibbett et al., 2011) and LS-Dyna (LSTC, 2013) are some of the mostly used commercially available programs. Polat and Bruneau (2017, 2018), Epackachi et al. (2015), Kurt et al. (2016) used LS-Dyna to replicate experimentally obtained wall behavior such as wall base shear–top displacement hysteresis. Most of the numerical studies conducted previously employed limited number of concrete material models. A comparative study using different concrete material models for C-PSW/CF is limited. It is of interest to investigate the wall behavior using other concrete material models available in the programs. The focus of the study is to evaluate the significance of different concrete material models by using a previously benchmarked planar C-PSW/CF with boundary elements. The concrete material models considered are Mat085 (Winfrith), Mat072R3 (KCC) and Mat159 (CSCM) (all available in LS-Dyna). These concrete models are popular in structural modeling and simple to use.

2. Description of Reference Wall

The reference wall under consideration is shown in Fig. 1(a-b), where part (a) shows the wall cross-section and dimensions, and; part (b) shows the partial elevation of the wall base. Note that this wall model is one of the four walls tested and experimentally investigated by Alzeni and Bruneau (2017) (referred as B2 in that study). (Note that, in those four wall models, two had full circular boundary elements, and two had half-circular boundary elements. This study aimed to study behavior a wall with full circular boundary elements — with no other selection criteria). The wall was cantilever type and had a length of 3048mm from the base. As shown in Fig. 1(a) the wall consisted of circular boundary elements (HSS sections with a diameter of 219mm and thickness of 7.94mm) and dual steel web plates extending between the boundary elements (web plates had a thickness of 7.94mm and a width of 203.2mm). The inside volume of the circular boundary elements and dual web plates were filled with concrete (the thickness of the concrete between the steel web plates was 152.4mm). Tie bars (having a diameter of 25.4mm) were used to connect the dual web plates in the transverse direction. The vertical and horizontal spacing of tie bars was 304.8mm.

3. Theoretical Wall Strength and Plastic Neutral Axis Location

C-PSW/CF is assumed, theoretically, to reach its plastic moment capacity which is defined based on the assumption of uniform uniaxial yield strength of steel and uniaxial compressive strength of concrete (AISC, 2016). Fig. 2 shows the wall cross-section along with the assumed uniform plastic stress distributions of the skin steel and concrete. For fully plastic stress distribution, the skin steel is assumed to reach yield stress of F_y in compression and tension, and the concrete is assumed to reach compression stress of f_c'. Plastic moment capacity of the wall is given by the summation of the moments of the compressive and tensile force vectors about wall plastic neutral axis. The tensile and compressive force vectors are denoted by T_1, T_2, C_1, C_2, C_3, C_4, C_5 and shown in Fig. 2. In Fig. 2, the wall plastic neutral axis is defined based on a parameter C which can be calculated by equilibrium of compressive and tensile force vectors.

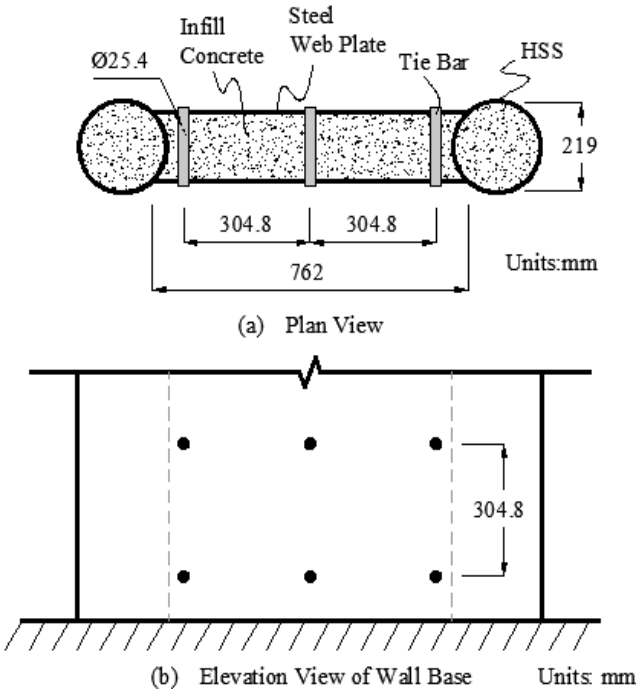

Fig. 1. Reference C-PSW/CF:
a) Plan view; b) Elevation view of wall base.

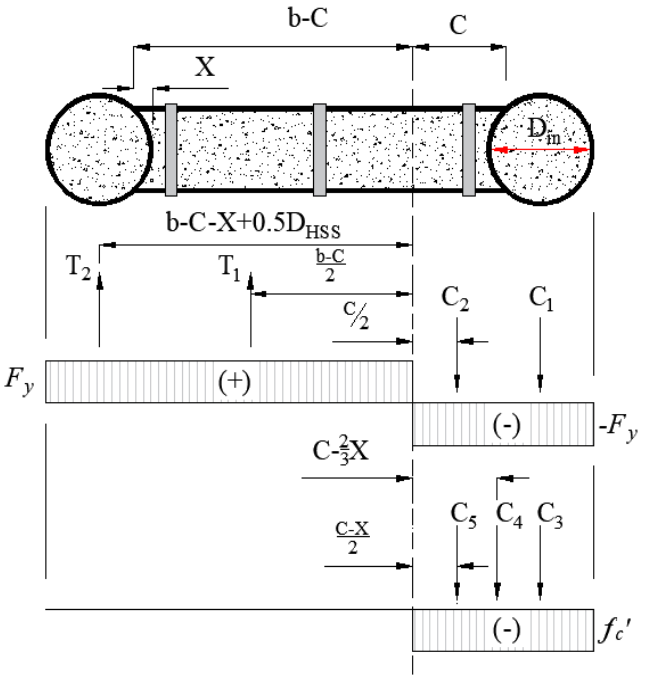

Fig. 2. Uniform stress distribution of steel and concrete part of the wall cross-section.

A closed-form solution for wall plastic moment, M_p, and plastic neutral axis, C, were provided by AISC (2016) and given in Eqs. (1) and (2). In these equations, A_{HSS} is the area of the HSS, F_{yHSS} and F_{yweb} are, respectively, the yield strength of the HSS and the steel web, d_{HSS} and d_{in} are, respectively, the outer and inner diameter of the HSS section, t_c and t_s are, respectively, the thickness of the infill concrete and steel. In Eq. (2), an auxiliary parameter, X, defined in closed form by Eq. (3), is used. Theoretical solutions using Eqs. (1) and (2) yield a value of M_p=3280 kN-m, and a C value of about 180mm. Including the partial depth of the HSS (≈180mm), a total compression depth is equal to about 360mm.

$$M_{pc} = M_n = A_{HSS}F_{yHSS}(b - 2X + d_{HSS}) + (b^2 + 2C^2 - 2Cb)t_sF_{yweb} + \left[0.25\pi d_{in}^2(0.5d_{HSS} + C - X) + 0.33Xt_c(C - 0.67X) + 0.5t_c(C - X)^2\right]f_c' \quad (1)$$

$$C = \frac{2bt_sF_{yweb} - \left(0.25\pi d_{in}^2 - 0.67Xt_c\right)f_c'}{4t_sF_{yweb} + t_cf_c'} \quad (2)$$

$$X = 0.5\left(d_{in} - \sqrt{d_{in}^2 - t_c^2}\right) \quad (3)$$

4. Finite Element Modeling of the Wall in LS-Dyna

Finite element modeling of the above-mentioned wall was previously developed by Polat and Bruneau (2017). Important modeling aspects are summarized as follows: shell, solid and beam elements were used to develop wall parts, namely; the steel plate, infill concrete and tie bars. Steel-concrete surface interaction was achieved by using a penalty-based contact model with interface friction (a coefficient of friction of 0.3 was used per the Coulomb friction model used by the contact model). Element sizes were determined based on a mesh convergence study. The size of the shell element was 25.4mm x 25.4mm and the solid elements was 25.4mm x 25.4mm x 25.4mm.

For modeling the concrete part of the wall, an eight-node constant stress solid element (Solid 1) with reduced integration was used. For modeling the steel part of the wall, a four node fully integrated shell element (Shell 16) with three integration points (through the thickness) was used. For modeling the ties, a two-node integrated beam element (Beam 1) was used. Fig. 3 shows the element mesh of the wall separately for the concrete infill (solid elements), tie bars (beam elements) and the steel skin (shell elements).

The material models used (as defined in LS-Dyna) in the finite element models were as follows: Mat 3, a bilinear material model with kinematic hardening, was used to define material properties of the steel plates and tie bars. The steel material properties used for the web plate and boundary elements (HSS) are as follows: Elastic modulus of E_s=205000MPa and 189000MPa, yield strength of F_y=441MPa and 386MPa, tangent modulus of E_t=100MPa and 413Mpa, respectively for the steel web plate and HSS. For tie bars, the same material model was used, except that F_y=345MPa and E=200000MPa. Three concrete material models, namely; Mat072R3 (Winfrith), Mat085 (KCC) and Mat159 (CSCM) were considered. The required input parameters with corresponding values for these concrete models are: concrete density of ρ=2.248e-008 N/mm^3, elastic modulus of 16,547 MPa, Poisson's ratio of 0.2, uniaxial concrete compressive strength of f_c'=49MPa, uniaxial tensile strength of f_t'= 4.9MPa and aggregate size of 7.9mm.

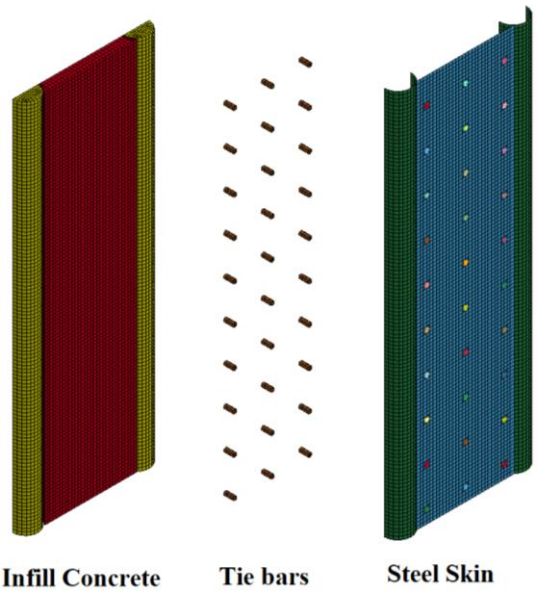

Fig. 3. Finite element model of the wall parts in LS-Dyna.

5. Comparison of Inelastic Cyclic Wall Responses

Cyclic wall responses were obtained by subjecting walls to displacement cycles at the wall top (displacement protocol was provided in Polat and Bruneau (2017)). Base moment – drift hysteresis, of the wall with different concrete material models were obtained and compared. Note that cyclic inelastic response of this wall was previously benchmarked by Polat and Bruneau (2017) using the Winfrith (Mat085) concrete model (in that study many wall response were successfully captured, such as; wall stiffness, strength and pinching). In this study, cyclic inelastic response of the same wall was investigated using the KCC and CSCM concrete models and the results are compared against the benchmarked results.

Figs. 4 and 5 show the comparison of the moment hysteresis curves obtained for the wall with the Winfrith, KCC and CSCM concrete models. As shown in Fig. 4, the moment hysteresis curve obtained using the KCC concrete model is in good agreement with that of the Winfrith concrete model in terms of wall stiffness and strength. As shown in Fig. 5 for the wall with the CSCM concrete model, wall strength and stiffness were over-predicted compared to those predicted using the Winfrith concrete model. The prediction of the wall pinching, however, was not captured successfully by the KCC and CSCM concrete models. Overall, the response obtained with the KCC concrete model is more reasonable than that obtained with the CSCM concrete model, and in better agreement with the benchmarked results obtained with using the Winfrith concrete model.

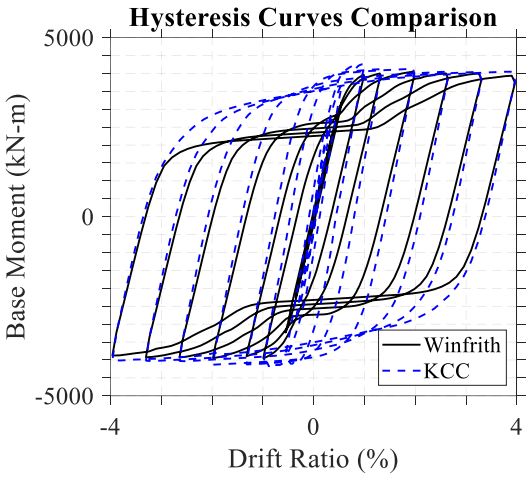

Fig. 4. Comparison of moment hysteresis of the wall with Winfrith and KCC concrete models.

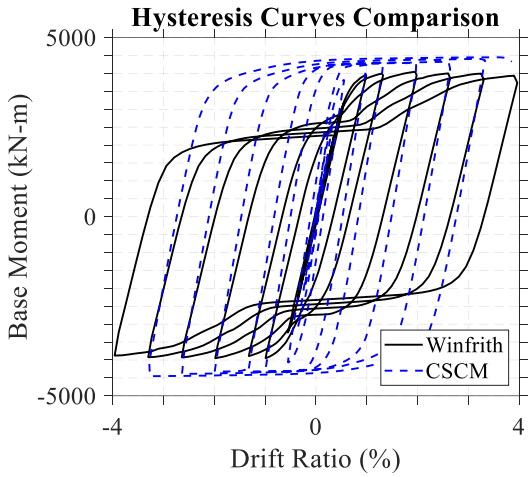

Fig. 5. Comparison of moment hysteresis of the wall with Winfrith and CSCM concrete models.

6. Investigation of Steel and Concrete Contribution to Total Wall Base Moment

Individual stiffness (lateral) and strength contribution of the steel and concrete of the wall models with the three concrete material models were investigated. Figs. 6-8 show the individual moment contribution of the steel (a), and concrete (b) to total base moment. Hysteresis curves in these figures show that contribution of the concrete and steel to total base moment varies for each concrete material model considered. For example, at 2.0% drift ratio steel contribution accounts for 73%, 64% and 63% of the total wall moment, while concrete contribution accounts for 27%, 36% and 37% of the total wall moment for the walls using the Winfrith, KCC and CSCM concrete models, respectively.

For the wall with the Winfrith concrete model (Fig. 6), the contribution of the steel to total wall strength is slightly reduced with increasing drift levels, whereas the contribution of concrete is slightly increased. This behavior is attributed to formation of local plate buckling on the steel web and HSS. Moreover, concrete contribution to stiffness is delayed as shown in Fig. 6(b) as a result of concrete cracking. Note that wall stiffness is related to wall pinching. Polat and Bruneau (2018) showed that wall pinching in flexural type C-PSW/CF was a result of concrete crack opening and closing. For the wall with the KCC concrete model (Fig. 7), similar to the wall with the Winfrith concrete model, there is slight reduction in steel strength and slight increase in concrete strength with increasing wall drift. Note that KCC concrete does not simulate concrete crack opening and closing therefore wall pinching cannot be captured with this material model. For the wall with the CSCM concrete model (Fig. 8), steel and concrete contribution to total wall moment differs from that of the walls with the Winfrith and KCC concrete models. For this wall the reduction in steel contribution and increase in concrete contribution with increasing wall drifts is more significant than that obtained using the Winfrith concrete model.

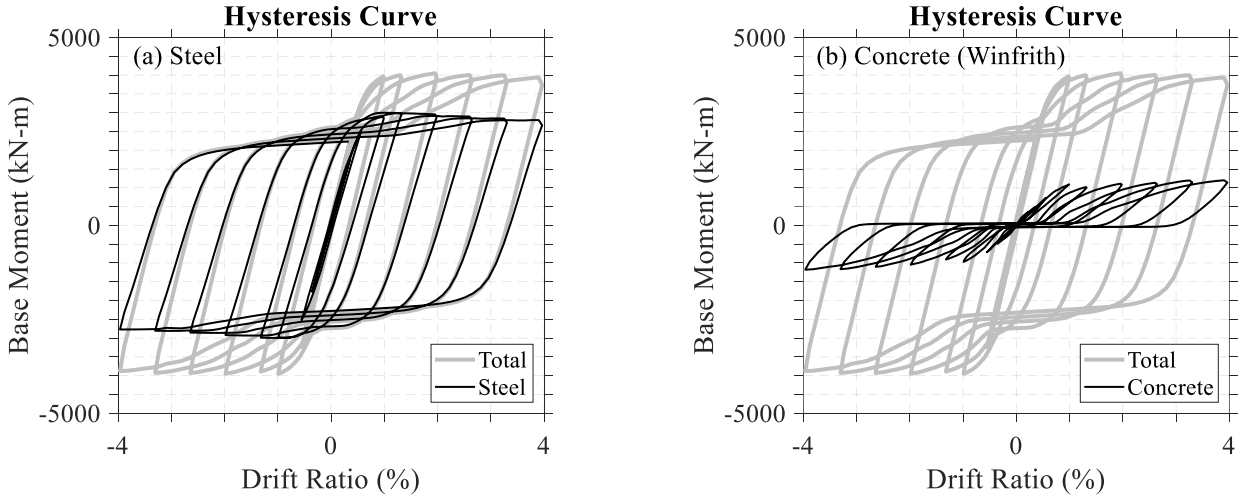

Fig. 6. Contribution of the wall parts to total base moment hysteresis of the wall with Winfrith (Mat085) concrete model: a) Steel; b) Concrete.

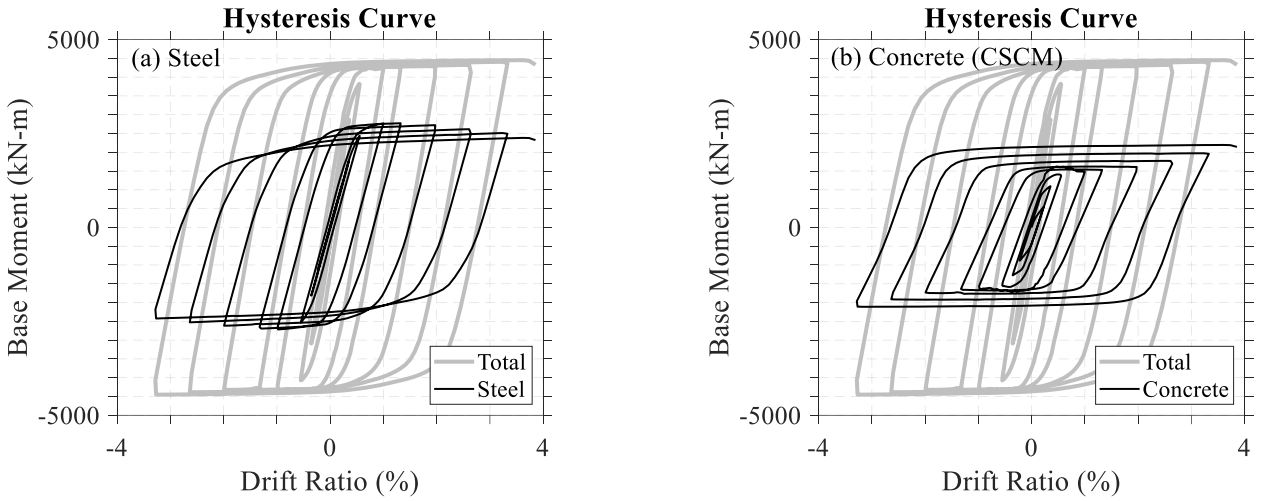

Fig. 7. Contribution of the wall parts to total base moment hysteresis of the wall with KCC (Mat072R3) concrete model: a) Steel; b) Concrete.

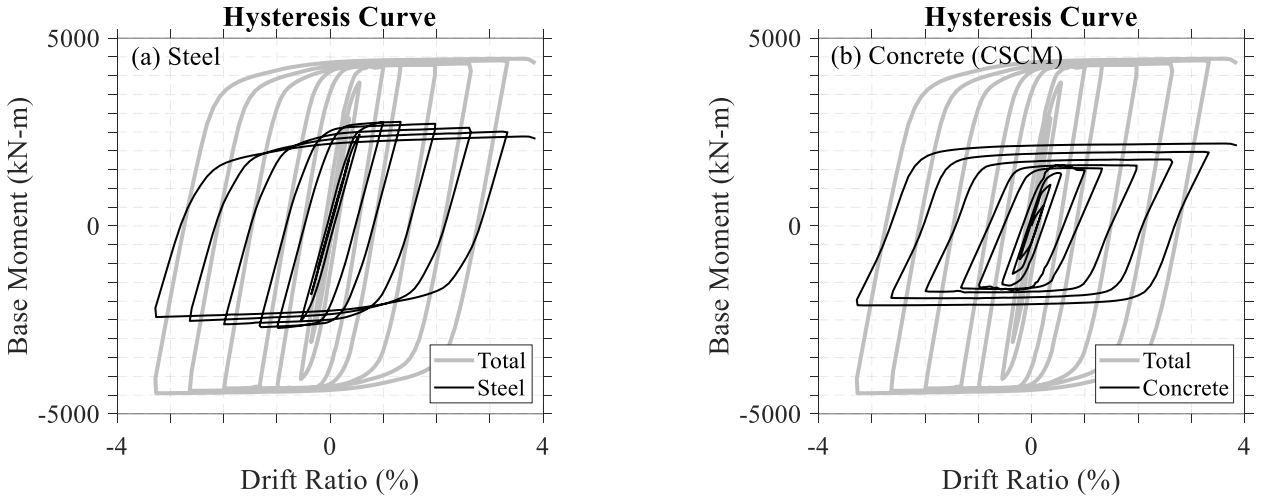

Fig. 8. Contribution of the wall parts to total base moment hysteresis of the wall with CSCM (Mat159) concrete model: a) Steel; b) Concrete.

7. Investigation of Moment Contribution of Wall Web and Boundary for Steel and Concrete

In flexural type shear walls, most of the moment demand is resisted by the boundary (outermost) region of the wall—while most of the shear force is mainly resisted by the wall web. The reference wall model under consideration has boundary elements in the form of full HSS and it is of interest to quantify individual contribution of the wall boundary and wall web regions of the steel and concrete parts to total base moment of the steel and concrete parts of the wall. In this section individual contribution of the steel web and steel boundary to total base moment of the total steel part (web and boundary), and contribution of concrete web and concrete boundary to total base moment of the total concrete part (web and boundary) of the wall were investigated for the walls using the three concrete models.

Figs 9-11 show the contribution of the wall steel (part (a) of the figures) and wall concrete (part (b) of the figures) to total base moment due to steel and concrete parts of the wall, respectively for the wall using the Winfrith, KCC and CSCM concrete material models. For all the walls with the three concrete material models considered, the steel boundary and the steel web account about 66% and 33% of the total moment contribution of the wall steel, respectively (i.e. at 2% drift ratio based on the results presented in part (a) of the figures). For the wall with the Winfrith concrete model, the concrete boundary and the concrete web account 74% and 26% of the total moment contribution of the wall concrete (per Fig. 9(b)). For the wall with the KCC concrete model, the concrete boundary and the concrete web account 97% and 3% of the total moment contribution of the wall concrete (per Fig. 10(b)). For the wall with the CSCM concrete model, the concrete boundary and the concrete web account 80% and 20% of the total moment contribution of the wall concrete (per Fig. 11(b)). Results indicate that for the wall with the KCC concrete, the concrete within the wall web has almost no contribution to wall moment. This indicates that neutral axis is close to the web-boundary interface region for this wall so that very little

amount of web concrete is under compression. For the wall with the Winfrith and CSCM concrete models, moment contribution of the web concrete is somewhat close to each other (26% vs. 20%). This indicates larger compression depth for these walls than obtained from the wall with KCC concrete model.

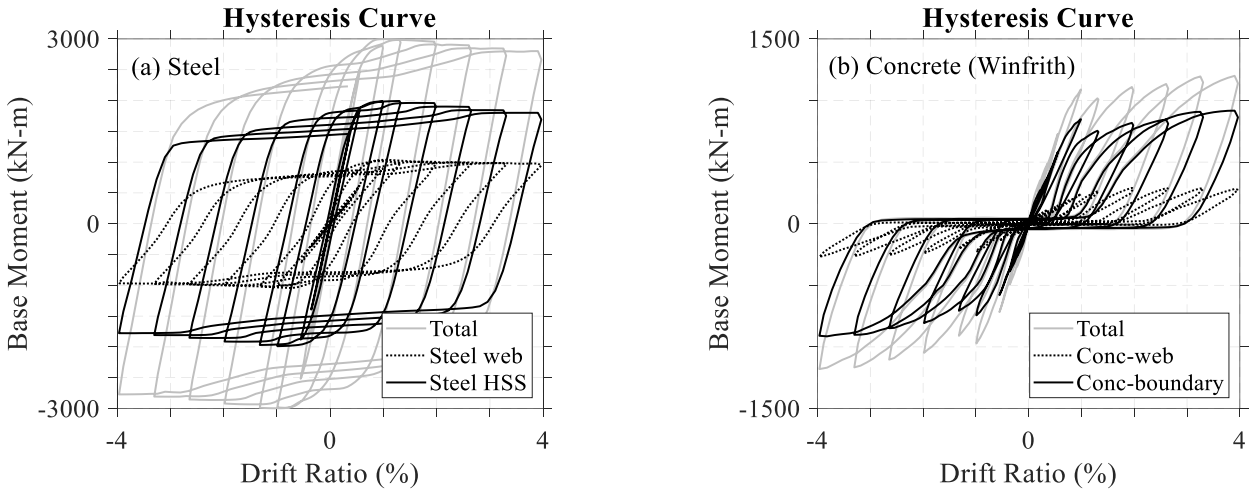

Fig. 9. Contribution of wall web and boundary elements to total base moment of the wall with Winfrith concrete model: a) Steel; b) Concrete.

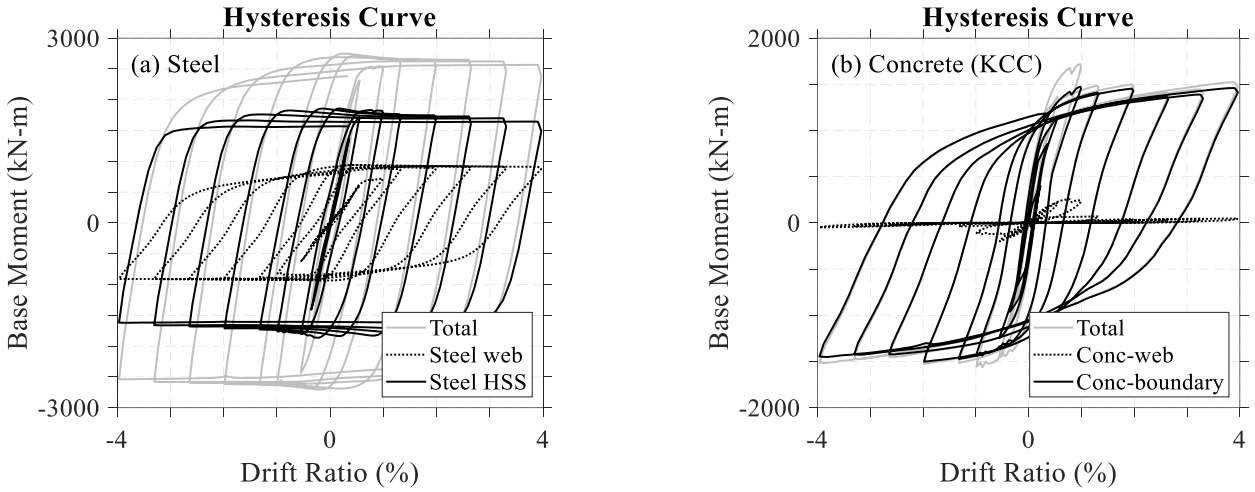

Fig. 10. Contribution of wall web and boundary elements to total base moment of the wall with KCC concrete model: a) Steel; b) Concrete.

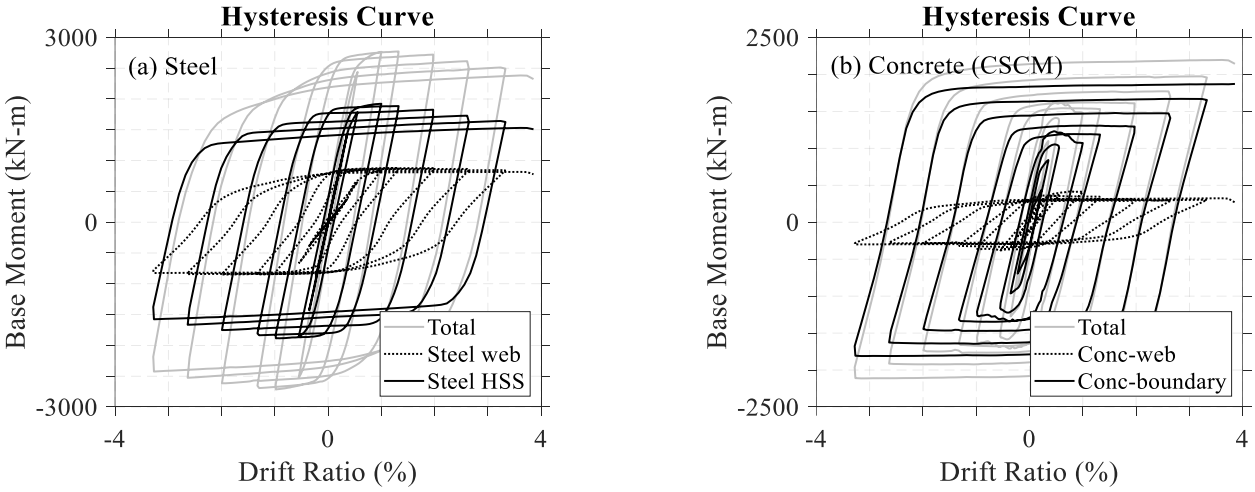

Fig. 11. Contribution of wall web and boundary elements to total base moment of the wall with CSCM concrete model: a) Steel; b) Concrete.

8. Comparison of Wall Neutral Axis and Concrete Axial Stress Distribution

Wall neutral axis obtained for the walls using the Winfrith, KCC and CSCM concrete models are compared. Axial stress contours of the infill concrete were plotted along the wall length at peak wall deformation for negative and positive values. This allowed comparison of the wall neutral axis, visually. For a quantitative comparison of the wall neutral axis and axial strength demand in the concrete, average axial stress distributions of the infill concrete at the wall base were obtained and plotted across the depth of the wall cross-section.

Fig. 12(a-c) shows negative and positive stress contours of the concrete of the walls using the Winfrith (a), KCC (b), and; CSCM (c) material models to show the wall neutral axis along the wall height. In this figure, compressive and tensile stresses are shown by two different colors (i.e., black and gray regions represent the compression and tension region of the wall, respectively). (Note that at larger drifts, the concrete under tensile stresses starts cracking – not shown in the figure – as such the compression depth is smaller than the half of the total depth). Focusing on the wall neutral axis at the wall base (highest axial strain region of the wall) the following observations can be made: the wall using the Winfrith concrete model exhibits slightly larger compression depth than that of the wall using KCC concrete model, and; slightly lower compression depth than that of the wall using CSCM concrete model.

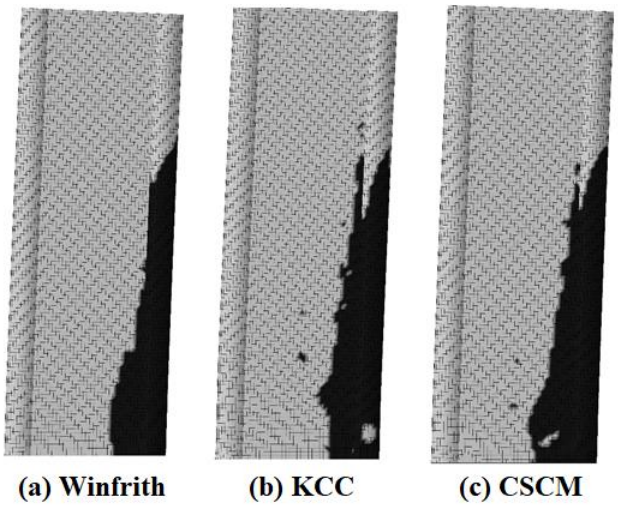

Fig. 12. Plastic neutral axis of the infill concrete of the walls with: a) Mat085, b) Mat072R3; c) Mat159.

Fig. 13 shows average axial stress distribution of the infill concrete obtained for wall using the Winfrith (a), KCC (b) and CSCM (c) concrete models at specified wall drifts of 0.25%, 0.5%, 1.0%, 1.5%, 2.0%, 2.5% and 3.0%. As shown in Fig. 13(a), for the wall with the Winfrith concrete model, maximum concrete strength was attained at the wall web. For example, the maximum average stress values of the concrete within the wall web is about 85MPa while the maximum averages stress values of the concrete core (inside the boundary element) is about 60MPa. The lower axial strength demand in the boundary element is attributed to possible slippage between the HSS and the concrete core (note that steel-concrete interaction of the boundary element is solely achieved by interface friction; i.e., no tie bars were used). As shown in Fig. 13(b), for the wall with the KCC concrete model, maximum concrete strength is attained at the wall boundary. For example, the value of the maximum average stress of the boundary concrete and web concrete are about 100MPa and 80MPa, respectively. As shown in Fig. 13(c), for the wall with the CSCM concrete model, maximum concrete strength is (similarly to the wall with the KCC concrete) attained at the boundary concrete having a maximum average stress of about 60MPa (note that, for this case, the average axial stress curves obtained are not as smooth as the curves obtained for the Winfrith and KCC concrete). Note that all the measured results exceed the unconfined uniaxial concrete compression strength of 49MPa which indicates some level of confinement of the concrete.

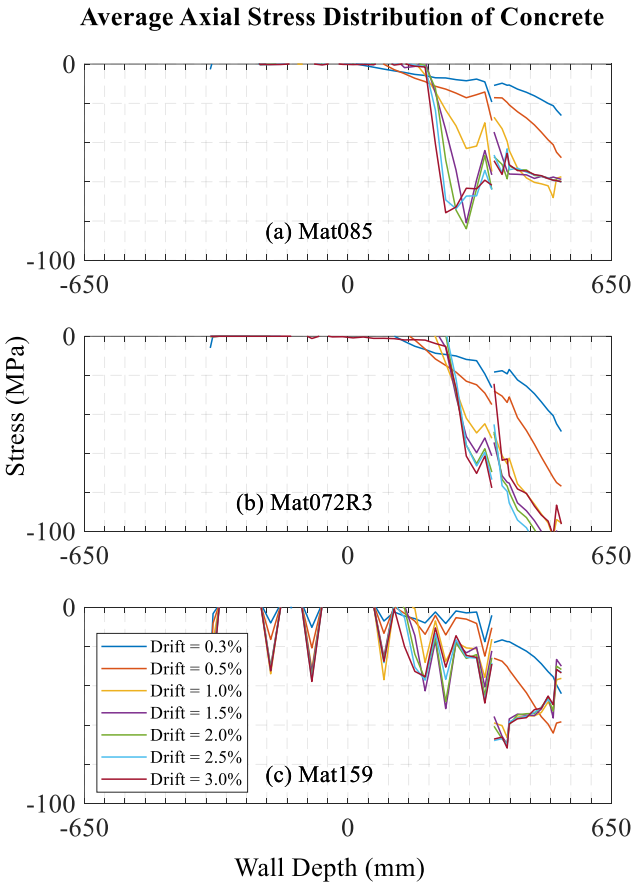

Fig. 13. Average axial stress distribution of concrete of the wall with: a) Mat085, b) Mat072R3; c) Mat159.

Fig. 13 reveals the compression depth of the wall models as a function of wall drifts. For example, it is shown that compression depth of the wall obtained using the Winfrith concrete model is slightly larger than that of the wall using the KCC concrete model, and lower than that of using the CSCM concrete model. From the figure, the predicted compression depth of the wall is about 350mm, 300mm and 450mm for the wall with the

Winfrith, KCC and CSCM concrete models, respectively. Recalling that the theoretically calculated plastic neutral axis was 360mm, the neutral axis, predicted by the numerical models, is less for the wall with KCC and higher for the wall with the CSCM concrete models.

9. Conclusions

Three concrete material models available in LS-Dyna, namely the Winfrith, KCC and CSCM, were used to investigate their influence on cyclic inelastic response of a previously benchmarked composite plates shear wall-concrete filled using LS-Dyna. Wall base moment hysteresis of the wall models using the three material models were obtained and compared. Results showed that wall lateral stiffness and strength prediction of the KCC concrete model was in good agreement with the previously benchmarked results for the wall using the Winfrith concrete model. Wall strength over-predicted by the CSCM concrete model. Both, the KCC and the CSCM concrete models could not capture the actual wall pinching.

Individual moment contributions of the steel and concrete showed for the wall with the KCC concrete model that, there is slight reduction in steel strength and slight increase in concrete strength with increasing wall drift. For the wall with the CSCM concrete model, the reduction in steel contribution and increase in concrete contribution with increasing wall drifts is more significant than that obtained using the Winfrith concrete model.

Investigation of moment contribution of wall web and boundary for steel and concrete showed for all the walls with the three concrete material models that, the steel boundary and the steel web account about 66% and 33% of the total moment contribution of the wall steel, respectively. On the other hand, contribution of the concrete web and concrete boundary to total moment contribution of the wall concrete varied for each of the concrete model used.

Investigation of wall neutral axis showed that, wall neutral axis obtained using the Winfrith concrete model is slightly larger than that obtained from the wall using the KCC concrete model and slightly smaller than that obtained from the wall using the CSCM concrete model. Average axial stress distribution of the concrete showed that maximum demand occurred at the wall web for the wall with the Winfrith concrete model; at the boundary element for the wall with the KCC and CSCM concrete models. For all the models, average axial stress values obtained were higher than the uniaxial unconfined compressive strength of the concrete, which indicated some level of confinement.

Publication Note

This research has previously been presented at the 8th International Symposium on Steel Structures held in Konya, Turkey, on October 25-26, 2019. Extended version of the research has been submitted to Challenge Journal of Structural Mechanics and has been peer-reviewed prior to the publication.

References

AISC (2016). Seismic provisions for structural steel buildings. *AISC 341-16*, AISC, Chicago.

Alzeni Y, Bruneau M (2017). In-plane cyclic testing of concrete-filled sandwich steel panel walls with and without boundary elements. *Journal of Structural Engineering*, 143(9), 04017115.

Epackachi S, Whittaker AS, Varma AH, Kurt EG (2015). Finite element modeling of steel-plate concrete composite wall piers. *Engineering Structures*, 100, 369-384.

Hibbett, Karlsson, Sorensen (2011). *ABAQUS/standard: User's Manual*. Dassault Systèmes Simulia, Providence, RI, USA.

Kurt EG, Varma AH, Booth P, Whittaker AS (2016). In-Plane behavior and design of rectangular SC wall piers without boundary elements. *Journal of Structural Engineering*, 04016026.

LSTC (2013). *Keyword User's Manual, Volume II, Material Models*, Livermore Software Technology Corporation (LSTC), Livermore, CA, USA.

Polat E, Bruneau M (2017). Modeling cyclic inelastic in-plane flexural behavior of concrete filled sandwich steel panel walls. *Engineering Structures*, 148, 63-80.

Polat E, Bruneau M (2018). Cyclic inelastic in-plane flexural behavior of concrete filled sandwich steel panel walls with different cross-section properties. *Engineering Journal, American Institute of Steel Construction*, 55, 45-76.

Varma AH, Shafaei S, Klemencic R (2019). Steel modules of composite plate shear walls: Behavior, stability, and design. *Thin-Walled Structures*, 145, 106384.